INELASTIC NEUTRON SCATTERING, EPR AND SPIN CHIRALITY IN SPIN-FRUSTRATED V_3 and Cu_3 NANOMAGNETS WITH DZIALOSHINSKY-MORIYA EXCHANGE

Moisey I. Belinsky

School of Chemistry, Tel-Aviv University, Tel-Aviv, Ramat Aviv 69978, Israel

Abstract. The inelastic neutron scattering (INS) and EPR transitions are considered for the spin-frustrated V_3 and Cu_3 nanomagnets. It is shown that the DM exchange and distortions determine the Q-dependence and redistribution of the intensities of the intra- and inter-doublet INS transitions in the 2(S=1/2) states as well as the intensities of the EPR transitions. The peculiarities of the INS and EPR spectra of the V_3 ring of V_{15} quantum molecular magnet and EPR spectra of the V_3 and Cu_3 nanomagnets are described by the isosceles Heisenberg model with the DM exchange. Spin chirality and spin structure of the Cu_3 and V_3 nanomagnets with the Dzialoshinsky-Moriya (DM) exchange interaction are analyzed in the vector and scalar spin chirality models. The vector chirality model describes the field, orientation and deformation dependence of the spin chirality κ_n. The spin chirality is formed by the DM interaction and depends on the sign of the DM parameter G_z. The DM exchange and distortions determine the degree of chirality κ_n<1 in the isosceles clusters.

1. Introduction

Metal clusters have attracted significant interest as molecular magnets [1], possible components for molecule-based quantum computation [2-4], as well as active centers of biological systems [5]. In the equilateral Cu_3 and V_3 clusters, (J_{ij}=J_0), the Heisenberg antiferromagnetic (J_0>0) exchange interaction $H_0=\sum J_0 \boldsymbol{S}_i\boldsymbol{S}_j$ leads to the spin-frustrated ground state 2(S=1/2) and excited S=3/2 state [6, 7]. These trinuclear clusters are the simplest magnetic systems which allow one to investigate the effects of the Dzialoshinsky-Moriya [8, 9] (DM) exchange $H_{DM}=\sum \boldsymbol{G}_{ij}[\boldsymbol{S}_i\times\boldsymbol{S}_j]$ and distortions, anisotropy of magnetic and spectroscopic characteristics [6, 7], the spin-frustration, spin chirality, spin reorientation, and quantum magnetization. Large DM exchange in the Cu_3 trimers with large J (>150 cm^{-1}) was found and described in the DM(z) model with the DM parameters G_z=5, 15-47 cm^{-1} (G_z/J_{av}=0.155-0.225) [6,7, 10-17]. For the equilateral clusters with large J_0, the DM exchange results in zero-field splitting (ZFS) $2\Delta_{DM}{}^0=|G_z|\sqrt{3}$ of the 2(S=1/2) ground state (GS), and determines the anisotropy of magnetic and spectroscopic characteristics [6, 7, 10-17]. In the isosceles DM clusters with $J_{13}=J_{23}\neq J_{12}$, the ZFS 2Δ of the 2(S=1/2) states is determined by G_z and δ-distortion [6, 7]. The DM mixing of the spin states in the Cu_3 clusters with large J and G, and the origin of the DM exchange parameters were considered in ref [18].

The DM exchange is also active in the clusters with small Heisenberg and DM parameters such as the {Cu_3} [19-21] and [V_3] [22] nanomagnets, as well as the V_3 ring of V_{15} quantum molecular nanomagnet [23-33, 2a]. These trimers with small J (J=1.7-3.4cm^{-1}=2.4-4.8K) have attracted much attention as molecular magnets [2a, 19-33]. The effect of quantum magnetization, owing to the spin-frustrated 2(S=1/2) doublets, was observed first in the V_3 ring of V_{15} [23, 24], and later in the [V_3] [22] and {Cu_3} [19, 20] nanomagnets. These clusters are characterized by the crossing of the |3/2,-3/2> and |1/2,-1/2> levels at level-crossing (LC) field H_{LC} ($H_{LC}=3J/2g\mu_B$) and tunneling gaps Δ_{ij} at H_{LC}. The ZFS, tunneling gaps, quantum magnetization and EPR spectra of the V_3 ring of V_{15} were explained in the equilateral DM model with the non-zero G_z and G_x, G_y parameters (G=0.05-0.2K) [23-33].

The microscopic origin of this 2Δ-gap of the spin-frustrated 2(S=1/2) states of the V_3 ring of V_{15} is a subject of discussion until now [33, 34]. The DM exchange coupling in the V_3 ring of V_{15} was proposed [23-33, 3a] for the explanation of the 2Δ-gap and quantum magnetization. On the other hand, this 2Δ-gap was described by the isotropic pure Heisenberg scalene triangle model ($J_{12}\neq J_{13}\neq J_{23}$) [34] on the basis of the observed inelastic neutron scattering (INS) spectra [34]. At the same time, recent EPR investigations [33] of the V_3 ring of V_{15} show the angle dependence of the resonance fields, which was discussed in the equilateral DM exchange model [33]. The correlations between the INS and EPR spectra, chirality and geometry of the V_3 clusters require the joint analysis of the INS and EPR spectra in the trimeric DM models. The influence of the DM exchange on the INS transitions was not considered in the Heisenberg spin models of the INS transitions [35-37].

The DM exchange, the ground state (GS) spin chirality and the tunneling gaps at LC field H_{LC}, play the principal role in explaining the quantum magnetization in the {Cu_3} [19, 20] and [V_3] [22] DM nanomagnets (G_n≈0.5K). The spin chirality in the {Cu_3} DM nanomagnets was proposed as the parameter for electric control over a single molecular spin system which allows manipulation with the spin triangles as elements for molecule-based quantum computation [19-21]. However, the spin chirality of the Cu_3 and V_3 clusters with the DM exchange, the correlation between chirality and tunneling gaps, the dependence of spin chirality on magnetic field and distortions were not considered.

The aim of the paper is the consideration of i) the INS and EPR transitions in the V_3 clusters with the DM exchange, and application of the DM exchange models for the explanation of the observed INS and EPR spectra of the V_3 and Cu_3 nanomagnets, and ii) the influence of the DM exchange on the spin chirality of the V_3 and Cu_3 nanomagnets, the field and deformation dependence of the spin chirality

2. The DM exchange splitting and mixing of spin states

The Hamiltonian of the distorted V_3 and Cu_3 clusters

$$H=(J_{12}\boldsymbol{S}_1\boldsymbol{S}_2+J_{23}\boldsymbol{S}_2\boldsymbol{S}_3+J_{13}\boldsymbol{S}_1\boldsymbol{S}_3)+H_{DM}+H_{ZFS}+\sum\mu_B\boldsymbol{S}_i\boldsymbol{g}_i\boldsymbol{H} \quad (1)$$

describes the isotropic Heisenberg exchange H_0, the DM exchange [8, 9]

$$H_{DM}=\sum\boldsymbol{G}_{ij}[\boldsymbol{S}_i\times\boldsymbol{S}_j], \quad (2)$$

ZFS of the S=3/2 state ($H_{ZFS}=D_0[S_Z^2-S(S+1)/3]$) and Zeeman interaction, *ij*=12, 23, 31.

In the equilateral cluster, the DM(z) coupling $H_{DM}(z)=\Sigma G_{ij,z}[\boldsymbol{S}_i\times\boldsymbol{S}_j]_z$ splits the spin-frustrated 2(S=1/2) states on the two doublets with the energy $E_{1,2}=-d_z$, $E_{3,4}=d_z$; $d_z=½G_z\sqrt{3}$ [6,7]. The spin eigenfunctions [$u_+(-1/2)$, $u_-(1/2)$] and [$u_-(-1/2)$, $u_+(1/2)$], which diagonalize the $H_{DM}(z)$ model in the representation φ_0, φ_1 of the intermediate spins (S_{12}=0 and 1 in $\varphi_{S_{12}}(S,M)$) are the following:

$u_+(-1/2)=|1,-1/2>=-[\varphi_0(-1/2)+i\varphi_1(-1/2)]/\sqrt{2}=i[|\downarrow\downarrow\uparrow>+\omega|\uparrow\downarrow\downarrow>+\omega^2|\downarrow\uparrow\downarrow>]/\sqrt{3}$, (3)

$u_-(+1/2)=|-1,1/2>=[\varphi_0(1/2)-i\varphi_1(1/2)]/\sqrt{2}=-i[[|\uparrow\uparrow\downarrow>+\omega|\uparrow\downarrow\uparrow>+\omega^2|\downarrow\uparrow\uparrow>]/\sqrt{3}$;

$u_-(-1/2)=|-1,-1/2>=[\varphi_0(-1/2)-i\varphi_1(-1/2)]/\sqrt{2}=i[|\downarrow\downarrow\uparrow>+\omega^2|\uparrow\downarrow\downarrow>+\omega|\downarrow\uparrow\downarrow>]/\sqrt{3}$,

$u_+(+1/2)=|1,1/2>=-[\varphi_0(1/2)+i\varphi_1(1/2)]/\sqrt{2}=-i[[|\uparrow\uparrow\downarrow>+\omega^2|\uparrow\downarrow\uparrow>+\omega|\downarrow\uparrow\uparrow>]/\sqrt{3}$.

$\omega=e^{2\pi i/3}$, up and down arrows represent the up and down spins, respectively, for S_i. In the case of the existence of the G_x, G_y and G_z DM parameters [18b], the correlations between the in-plain components G_x, G_y of the DM vectors $\boldsymbol{G}_{ij}$ in the pair X_{ij}, Y_{ij}, Z_{ij} and the cluster *X, Y*, Z right-handed coordinate system have the form

$$G_{12,X}=G_{12,X_{12}}=G_x, G_{12,Y}=G_{12,Y_{12}}=G_y, \quad G_{23,X}=-½(G_x+\sqrt{3}G_y),$$
$$G_{23,Y}=½(\sqrt{3}G_x-G_y), G_{31,X}=-½(G_x-\sqrt{3}G_y), G_{31,Y}=-½(\sqrt{3}G_x+G_y). \quad (4)$$

The pair DM parameters are equal in the equilateral system, $G_{ij,X_{ij}}=G_x$, $G_{ij,Y_{ij}}=G_y$.

The *Z* components of the pair $\boldsymbol{G}_{ij}$ DM vector parameters are oriented perpendicular to the plain of the cluster $G_{12,Z}=G_{23,Z}=G_{31,Z}=G_z$, Z_{ij}||Z. The in-plain (G_x, G_y) DM exchange results in the mixing of the S=1/2 and S=3/2 states [25, 27-33, 18-22], which plays significant role in the V_3 and Cu_3 nanomagnets [18-33]. The group-theoretical analysis of the DM mixing in the V_3 ring of V_{15} was considered in refs [30, 31]. The matrix elements of the DM exchange mixing of the S=1/2 and Φ(3/2) states have the form

$$<u_\pm(\pm1/2)||\Phi(\pm3/2)>=(3i\sqrt{2}/4)G_\pm, <u_\pm(\mp1/2)||\Phi(\pm1/2)>=(i\sqrt{6}/4)G_\pm,$$
$$<u_\pm(\mp1/2)||\Phi(\mp3/2)>=0, \quad <u_\pm(\pm1/2)||\Phi(\mp1/2)>=0. \quad (5)$$

where $G_\pm=(G_x\pm iG_y)/\sqrt{2}$. The energy levels of the equilateral [V_3] cluster (J=4.8K, G_z=-0.5K, G_x=0.5K, G_y=0), the spin chirality, ZFS, and the DM mixing are shown in Fig.1, H=H_z. The lowest zero-field (ZF) state for G_z<0 is the [$u_-(-1/2)$, $u_+(+1/2)$] doublet. The DM exchange (G_x) results in the tunneling gap Δ_{12}' in the ground branch at LC field H_{LC1} and simple level crossing (Δ_{23}'=0) in the excited state at H_{LC2} for G_z<0, Fig. 1.

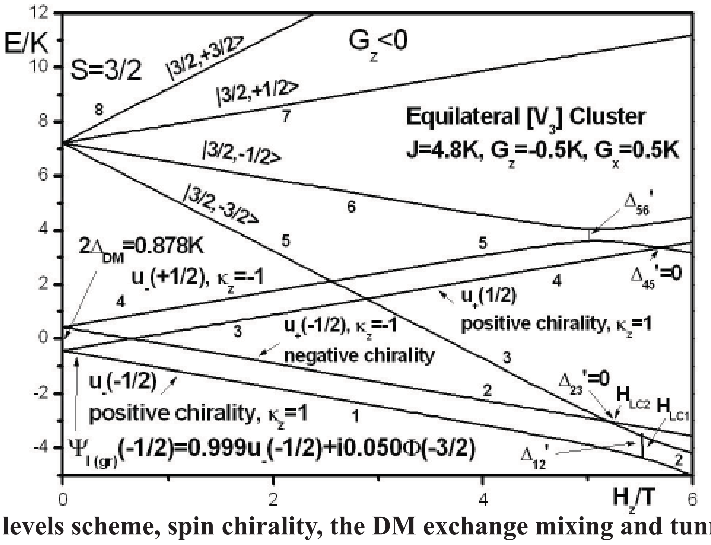

Fig. 1. The energy levels scheme, spin chirality, the DM exchange mixing and tunneling gaps in the equilateral V_3 cluster. J=4.8K, G_z=-0.5K, G_x=0.5K, G_y=0.

The isosceles $\{Cu_3\}$ nanomagnets [19, 20] with small J (J_{12}= 4.52 K, J_{13}=J_{23}=4.04 K) were characterized by the strong in-plain and out-of-plain DM(x,y,z) exchange coupling $|G_z|=G_x=G_y$=0.53K; G_z/J_{av}=0126, G/J_{av}=0.218 [20]. Fig. 2 shows the energy levels scheme, tunneling gaps, the INS and EPR transitions for this Cu_3 nanomagnet with different G_z parameters: G_z= +0.53K (dashed lines) and G_z=-0.53K (solid lines), g_{av}=2.06. For H<2T, the splittings do not depend on the sign of G_z. The in-plain (G_x, G_y) DM spin mixing results in the large tunneling gap Δ_{12}' in the ground branch at LC field H_{LC1} and small tunneling gap Δ_{23}' at H_{LC2} in the excited state for G_z<0, Fig. 2, solid. In the case G_z>0, small tunneling gap Δ_{12}' in the ground branch at LC field H_{LC1} and large tunneling gap Δ_{23}' in the excited branch at H_{LC2} take place, Fig. 2, dash.

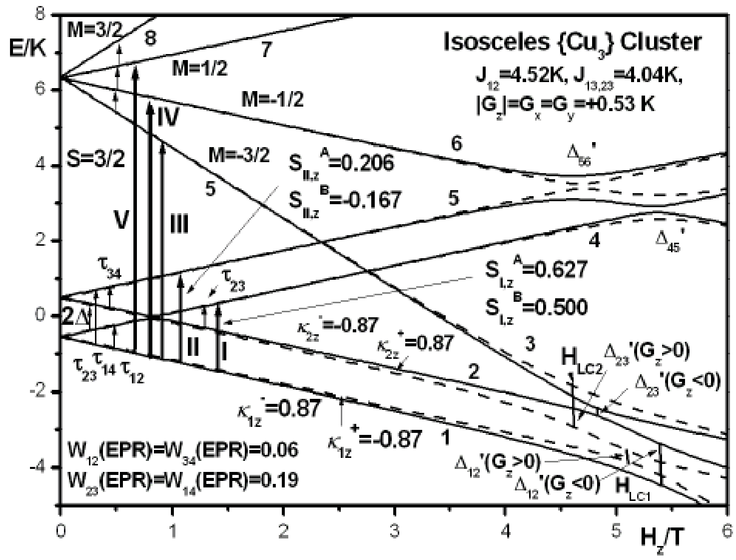

Fig. 2. Spin levels, the INS and EPR transitions, tunneling gaps in the isosceles Cu_3 nanomagnet.

3. Intensities of INS transitions in isosceles clusters with DM exchange

The expressions for the differential magnetic cross-section of INS, the intensities of the INS transitions in the Heisenberg clusters were presented in refs [34-37]. The INS transitions are determined by the spin structure factors $S_N(\mathbf{Q})$ [36], where $\boldsymbol{Q}$ is the scattering vector. The scheme of the INS transitions for the V_3 and Cu_3 isosceles nanomagnets is shown in Fig. 2. The analysis [34] of the observed INS transitions in the V_3 ring of V_{15} in the scalene Heisenberg model (G_n=0) results in the intensity ratios (III:IV:V)=3:2:1 for the transitions III, IV and V (Fig. 2). The Q-dependence of these transitions was described [34] very well by the equations I_{III}=1/2[1-sin(QR)/QR], I_{IV}=1/3[1-sin(QR)/QR], I_V=1/6[1-sin(QR)/QR], $I_{III}+I_{IV}+I_V$~[1-sin(QR)/QR]. For description of the Q-dependent intensity of the intra-doublet INS transition I (Fig. 2) of a scalene trimer with ground state $\Omega_0(\pm1/2)= a\varphi_0(\pm1/2)+b\varphi_1(\pm1/2))$, the equation $I_I=I_0F^2(Q)$ $[a^2+⅓b^2(1\text{-sin(QR)/QR})]$ was proposed [34].

The consideration of the spin structure factors shows that the scalene Heisenberg model (G_n=0) cannot describe the Q-dependence of the INS transition I [39]. The analysis of the INS and EPR spectra requires the taking in account the DM exchange.

The calculations of the INS for the isosceles DM trimer result in the structure factors for the INS transitions I-V (Fig. 2) in magnetic field $H=H_z$

$$S_I' = 1/2+(G_z^2/8\Delta^2)\,[1-4\cos(\mathbf{QR}_{23})], \tag{6}$$
$$S_{II}' = 1/3[1-\cos(\mathbf{QR}_{12})]-(G_z^2/8\Delta^2)\,[1-4\cos(\mathbf{QR}_{23})],$$
$$S_{III}' = 1/2[1-\cos(\mathbf{QR}_{12})],\ S_{IV}' = 1/3[1-\cos(\mathbf{QR}_{12})],\ S_V' = 1/6[1-\cos(\mathbf{QR}_{12})],$$

$\Delta=(\delta^2+d_z^2)^{1/2}=½[(J_{12}-J_{23})^2+3G_Z^2]^{1/2}$. The structure factors for the transitions I and II at high field H⊥Z are reduced to their values in the pure Heisenberg model, since high transverse magnetic field $H_\perp$ suppresses the effect of the DM exchange. The average structure factors $S_{N,av}'= S_N'$ for the INS transitions in the IS trimer have the form:

$$S_I'= 1/2+(G_z^2/24\Delta^2)\,[1\text{- }4\sin(QR)/QR], \tag{7}$$
$$S_{II}'=1/3[1-\sin(QR)/QR]-(G_z^2/24\Delta^2)[1-4\sin(QR)/QR],$$
$$S_{III}'=1/2[1-\sin(QR)/QR],\ S_{IV}'=1/3[1-\sin(QR)/QR],\ S_V'=1/6[1-\sin(QR)/QR].$$

In the absence of the DM exchange (G_z=0), the structure factor S_I' (7) of the INS transition I (Fig. 2) is reduced to the Q-independent form S_I'=1/2; the structure factor S_{II}' (7) of the INS transition II is reduced to S_{II}'=1/3[1-sin(QR)/QR], the structure factors of the Heisenberg isosceles trimer. Eq (7) shows significant influence of the DM exchange on the intensities of the intra-doublet transition I (S_I= $[S_I^A-S_I^B\sin(QR)/QR)$ and doublet-doublet transition II (S_{II}' =$[S_{II}^A-S_{II}^B\sin(QR)/QR]$). Thus, the S_I^B term of the DM exchange origin $S_I^B=\Delta S_I^B=(G_z^2/6\Delta^2)$ (7) results in the Q-dependence of the transition I [$S_I^B=S_{I,0}^B+\Delta S_I^B$, $S_{I,0}^B=0$]. The DM exchange switches on and increases the Q-dependence of the INS transition I and, at the same time, decreases the Q-dependence of transition II. The redistribution of the intensities of the INS transitions II and I, which is controlled by the DM exchange and distortions (the $[G_z/\Delta]^2$ term in (7)), takes place with the conservation rule $S_I^A+S_{II}^A=S_{I,0}^A+S_{II,0}^A$ for the Q-independent terms, and $S_I^B+S_{II}^B=S_{I,0}^B+S_{II,0}^B$ for the Q-dependent terms.

Calculated values of the S_I^A, S_{II}^A and S_I^B, S_{II}^B coefficients of the Q-independent and Q-dependent terms, respectively, of the averaged structure factors $S_I'=S_I^A-S_I^B\sin(QR)/QR$ and $S_{II}'=S_{II}^A-S_{II}^B\sin(QR)/QR$ of the INS transitions I and II, are shown in Fig. 2 for the set of the Heisenberg and DM parameters of the Cu_3 nanomagnet, which were determined [19, 20] in the magnetization and EPR experiment. The values of the structure factors in Fig. 2 [$S_{Iz}^A=0.627$ ($S_{I0}^A=0.5$), $S_{Iz}^B=0.500$ ($S_{I0}^B=0$); $S_{IIz}^A=0.206$ ($S_{II0}^A=0.333$), $S_{IIz}^B=-0.167$ ($S_{II0}^B=+0.333$)] show significant influence of the DM exchange on the intensities of the INS transitions.

The Q-dependence of the transitions I and II allows one to experimentally determine the $|G_z/2\Delta|$ relation. Thus, the experimentally observed Q-dependence of the transition I in the V_3 ring of V_{15} was described [34] by the Q-independent term ($a^2+b^2/3$)=0.6) and Q-dependent term [$-0.2\sin(QR)/QR$] [34]. For case, where the Q-dependence of the INS transition I is determined by Eq (7), the comparison with the coefficient [$(G_z/\Delta)^2/6$] in the Q-dependent term in S_I' (7) leads to the estimate $G_z/2\Delta\approx0.55$. Since $2\Delta\approx0.31$K and $J_{av}=2.46$K [34], this estimate results in $G_z\approx0.17$K and $\delta=0.06$K. In this case, the Q-independent term in the structure factor S_I' (7) of transition I is $S_I^A\approx0.55$. This value is close to the Q-independent term 0.6 for I in [34], that allows one to explain qualitatively the observation [34] that the overall intensity of peak I is significantly smaller than the sum of (III+IV+V).

In the isosceles [V_3] clusters, the DM exchange results in i) the Q-dependence of the spin structure factor S_I of the INS intra-doublet transition I (the coefficient S_I^B in S_I) and ii) the redistribution of the Q-independent S_I^A and S_{II}^A parts, as well as the Q-dependent, S_I^B and S_{II}^B, parts of the intensities of the INS transitions I and II with the conservation of the summary intensities of these two transitions: $S_I^A+S_{II}^A=S_{I,0}^A+S_{II,0}^A=5/6$ {$S_I^B+S_{II}^B=S_{I,0}^B+S_{II,0}^B=1/3$}.

4. EPR transitions in isosceles clusters with DM exchange

In the pure Heisenberg isosceles model, only intra-doublet 1→2(3) and 3(2)→4 EPR transitions are allowed for $H=H_z\|Z$ and $H(\perp Z)=H_\perp$ ($W_{1\to2(3)}=W_{3(2)\to4}=0.25$, $W_{14}=W_{23}=0$). For the isosceles trimer with the DM exchange, the relative intensities of the allowed EPR transitions (τ_{13}, τ_{24}, τ_{23}, τ_{14} in Fig. 2, $\hbar\nu>2\Delta$) for $H=H_z$ are determined by the equation $W_{13}=W_{24}=\delta^2/4\Delta^2$; $W_{14}=W_{23}=d_z^2/4\Delta^2$ [6, 7]. At high transverse magnetic field, $h_x>>\Delta$, the effect of the DM exchange is suppressed: $W_{13,x}'=W_{24,x}'=0.25$, $W_{14,x}=W_{23,x}=0$. Fig. 3 shows the frequency dependences [(ν_{ij}/γ_g)-H] of the resonance fields for the 2(S=1/2) states of the isosceles trimer with the DM exchange, $\gamma_g=g\mu_B/\hbar$.

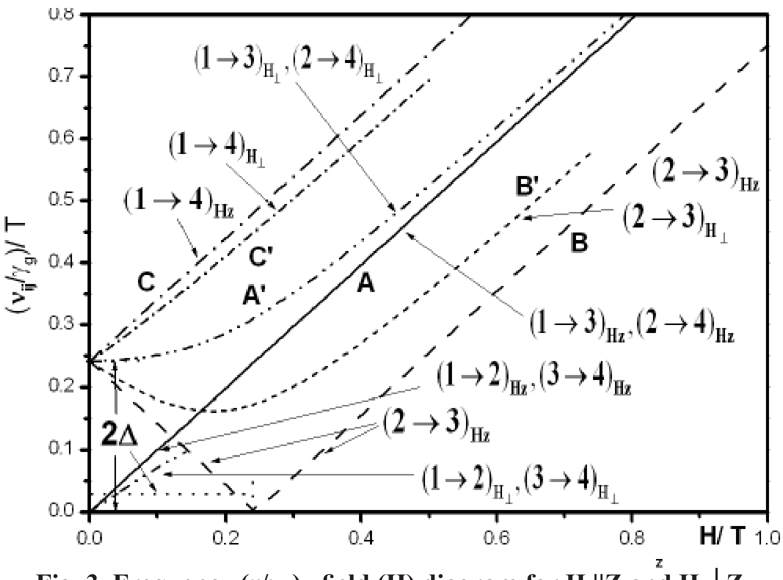

Fig. 3 Frequency (ν/γ_g) –field (H) diagram for $H_z\|Z$ and $H_x\perp Z$.

The straight A (solid), B (dash), and C (dash-dot) lines show the resonance conditions for the transitions $(1\to3)_{Hz}$, $(2\to4)_{Hz}$ [$W_{13,Hz}'=W_{24,Hz}'=0.14$] for $\hbar\nu>2\Delta_{SC}$ {$(1\to2)_{Hz}$, $(3\to4)_{Hz}$ (for $\hbar\nu<2\Delta_{SC}$)}, $(2\to3)_{Hz}$ and $(1\to4)_{Hz}$, [$W_{23,Hz}'=W_{14,Hz}'=0.11$], respectively, at magnetic field $H_z\|Z$. The A′ (dash-dot-dot) {B' (shot dash)} [C' (shot dash-dot)] curve shows the resonance conditions for the resonance fields for the EPR transitions $(1\to3)_{Hx}$, $(2\to4)_{Hx}$ {$(2\to3)_{Hx}$} [$(1\to4)_{Hx}$] at magnetic field $H\perp Z$. The non-linear field dependence A′, B′ (Fig. 3) of the frequency dependences ν(H) of the resonance fields at magnetic field $H\perp Z$ is characteristic for the DM exchange in the trimer. The low-frequency

EPR spectra [33] of the V_3 ring of V_{15} quantum molecular magnet were explained by the authors [33] in the equilateral DM model. The inter-doublet EPR transitions 1→4 and 2→3 and the intra-doublet 1→3 and 2→4 transitions with weak intensity for $H=H_z$ were observed in [33] (Fig. 2b[33]), as well as the linear magnetic behavior of the resonance frequencies for H||Z and non-linear magnetic behavior at H⊥Z (Fig. 2a [33]) induced by the DM exchange. The observation of the inter-doublet $(1\to4)_z$ and $(2\to3)_z$ EPR transitions and linear {non-linear} ν-H magnetic behavior for H||Z {H⊥Z} is the evidence of the presence of the DM exchange in V_3 ring (Fig. 2. B,C {A′}). At the same time, the intra-doublet low-frequencies $(1\to3)_z$ and $(2\to4)_z$ transitions are forbidden for the equilateral DM model and are allowed for the isosceles V_3 ring, Figs. 2, 3 ($W_{13}=W_{24}=\delta^2/4\Delta^2$). The observation of the τ_{13z}, τ_{24z} as well as the τ_{14z}, τ_{23z} EPR transitions on the V_3 ring of V_{15} [33] shows that this V_3 ring has the symmetry of the isosceles triangle (not equilateral) with the DM exchange. The observed correlation ($W_{13}\approx W_{24}<W_{14}\approx W_{23}$) between the intensities of the EPR transitions [33] corresponds to the relation $\delta<G_z\sqrt{3}$ in the isosceles DM model. The analysis of the calculated INS and EPR transitions [39] for the equilateral V_3 cluster and comparison with the observed INS [34] and EPR [33] transitions shows that the equilateral DM model cannot describe the EPR and INS spectra of the V_3 ring of V_{15}, the isosceles δ-distortion should be included in the consideration. The EPR spectra of the V_3 [22] and Cu3 [19, 20] nanomagnet also are described in the isosceles DM model.

5. Spin chirality of the Cu_3 and V_3 nanomagnets with DM exchange

Recently, the spin chirality of the {Cu_3} DM nanomagnet was proposed as the parameter for the manipulation with the spin triangles as units for molecule-based quantum gates [19-21]. The spin chirality of the magnetic systems is usually considered in the scalar chirality model and in the vector chirality model. The spin chirality in the {Cu_3} nanomagnet was considered [21], using the scalar chirality operator C_z

$$C_z = (4/\sqrt{3})\mathbf{S}_1\cdot[\mathbf{S}_2\times\mathbf{S}_3]. \tag{8}$$

The matrix elements of $\boldsymbol{C}_z$ in the $u_\pm(\pm1/2)$ basis (3) have the form

$$\chi_+ = <u_+(\pm1/2)\,|\,\hat{C}_z\,|\,u_+(\pm1/2)>=1, \qquad \chi_- = <u_-(\pm1/2)\,|\,\hat{C}_z\,|\,u_-(\pm1/2)>=-1. \tag{9}$$

The operator C_z splits the 2(S=1/2) set on the states $u_+(M_S)$ and $u_-(M_S)$ characterized by the projections $M_L=\pm1$ of the pseudoorbital moment L and does not act on the spin moments M_S, $M_S=\pm1/2$. The scalar chirality $\chi=\pm1$ pseudospin coincides with $M_L=\pm1$.

In the case of the vector chirality [38] which can be defined for the $S_i=1/2$ trimer as

$$\boldsymbol{K}_z=(2/\sqrt{3})\{[\mathbf{S}_1\mathrm{x}\mathbf{S}_2]_z+[\mathbf{S}_2\mathrm{x}\mathbf{S}_3]_z+[\mathbf{S}_3\mathrm{x}\mathbf{S}_1]_z\}, \tag{10}$$

the chirality vector $\boldsymbol{K}_z$ is parallel to Z-axis with amplitude +1 or -1, since the matrix elements of $\boldsymbol{K}_z$ in the $u_\pm(\pm1/2)$ basis have the form

$$\kappa_z = <u_\pm(\pm1/2)\,|\,\hat{\mathbf{K}}_z\,|\,u_\pm(\pm1/2)>=1, \qquad \kappa_z = <u_\pm(\mp1/2)\,|\,\hat{\mathbf{K}}_z\,|\,u_\pm(\mp1/2)>=-1. \tag{11}$$

The chirality is the sign of the projection of the spin vector onto the orbital momentum vector: negative is left, positive is right. In the positive (right) chiral states $u_+(1/2)$ and $u_-(-1/2)$ with $\kappa_z=+1$ (11), the direction of the spin moment (M_S) coincides with the direction of the pseudoorbital moment (M_L): thus, $M_L=-1$, $M_S=-1/2$, and the total pseudoangular moment is $M_J=M_L+M_S=-3/2$ for $u_-(-1/2)$; $M_L=+1$, $M_S=+1/2$, $M_J=M_L+M_S=3/2$ for $u_+(1/2)$. In the negative (left) chiral states $u_+(-1/2)$ and $u_-(1/2)$, $\kappa_z=-1$, the directions of M_S and M_L are opposite: thus, $M_L=-1$, $M_S=1/2$, $M_J=-1/2$ for $u_-(1/2)$; for $u_+(-1/2)$ - $M_L=+1$, $M_S=-1/2$, $M_J=+1/2$. The two states with M=-1/2 in Fig. 1 posses different vector spin chirality: In the case $G_z<0$, the GS is the positive (right) chiral state $u_-(-1/2)$, $\kappa_z=+1$, $M_L=\chi_{1z}^-=-1$, which exhibits the in-plain (G_x, G_y) DM exchange repulsion from the |3/2, -3/2> state that results in the tunneling gap Δ_{12}' at LC field H_{LC1} in the ground branch, Fig. 1. The first excited negative chiral state $u_+(-1/2)$, $\kappa_z=-1$ does not exhibit the DM mixing with the |3/2,-3/2> state, that results in the simple crossing ($\Delta_{23}'=0$) at H_{LC2}, Fig. 1. The equilateral trimers with $G_z>0$ and left chiral GS $u_+(-1/2)$, $\kappa_z=-1$, $\chi_{1z}^+==1$, posses the simple crossing ($\Delta_{12}'=0$) at LC field H_{LC1} in the ground branch and the tunneling gap Δ_{23}' at LC field H_{LC2} in the excited state. These correlations are consistent with the results of the group-theoretical analysis [30].

The DM exchange H_{DM} forms the chiral states of the DM trimer, the sign of G_z determines the vector spin chirality κ_z of the ground and excited states. The spin chirality of the pure Heisenberg states ($G_{ij}=0$) is equal to zero.

Fig. 4 shows the spin chirality κ_1 of the ground state and κ_2 of the first excited state of the equilateral V_3 cluster with the exchange parameters $J_0=4.8$K, $G_z=\pm0.5$K, $G_{x,y}=0$, in magnetic field $H=H_z||Z$ (κ_{1z}) and $H=H_x\perp Z$ (κ_{1x}, κ_{2x}). κ_{1n}^+ and κ_{1n}^- correspond to $G_z>0$ and $G_z<0$, respectively. The spin chirality in the DM(z) model (Fig. 4, short-dash-dot) does not depend on H_z for $H_z<H_{LC}$: i) $\kappa_{1z,0}^-=+1$ for the positive chiral ground state $u_-(-1/2)$, $G_z<0$, and ii) $\kappa_{1z,0}^+= -1$ for the negative chiral ground state $u_+(-1/2)$, $G_z>0$.

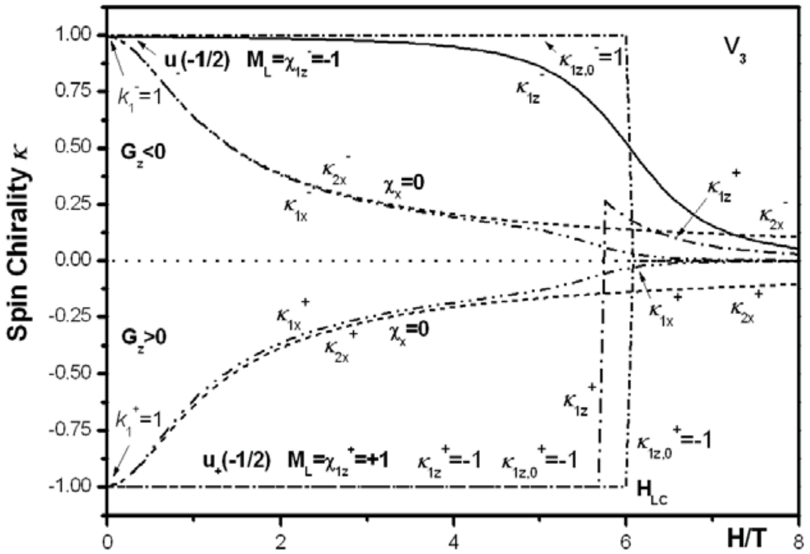

Fig. 4 Field dependence of the spin chirality of the equilateral V_3 cluster.

Chirality $\kappa_{1z,0}$ changes sharply to the value κ_{1z0} =0 (M_{gr}=-3/2) at LC field H=H_{LC}. Fig. 4 also shows the field dependence of the spin chirality of the V_3 cluster (J_0=4.8K, G_z=±0.5K) with the in-plane (G_x=0.5K) DM mixing. Positive chirality κ_{1z}^-=+1 of the ground u_-(-1/2) state (G_z<0) changes smoothly to the value κ_{1z}=0 after the avoided crossing (Fig. 4) due to the G_x DM mixing in accord with Fig. 1. In the case G_z>0, G_x≠0, negative chirality κ_{1z}^+=-1 of the ground u_+(-1/2) state is field-independent for H_z<H_{LC} and then κ_{1z}^+ changes abruptly at H_{LC} (Fig. 4) due to the simple level crossing. The states of the different vector chirality $\boldsymbol{\kappa}$ are characterized by the same scalar χ pseudospin: u_-(1/2), κ_z=-1, χ=-1 and u_-(-1/2), κ_z=+1, χ=-1.

In the case of the transverse field H_x⊥Z, the vector chirality operator K_z describes the projection of the spin chirality vector on the magnetic field. Eq (12) describes the field dependence $\kappa_{1x}(H_x)$ and $\kappa_{2x}(H_x)$ of the vector spin chirality of the ground and first excited states

$$\kappa_{1x} = \kappa_{2x} = \pm |\, d_z \,| / \sqrt{d_z^2 + h_x^2}\,, \tag{12}$$

the sign + (-) corresponds to G_z<0 (G_z>0), h_x=½g$\mu_B H_x$, Fig. 4. In the case G_z<0, the ZF chirality of the ground and first excited states (10) is positive and equal to 1: κ_{1x}^-= κ_{2x}^-=1, as in the field H_z, Fig. 4. In the case G_z>0, the ZF chirality is negative κ_{1x}^+= κ_{2x}^+= -1, Fig. 4. In the DM(z) model, the vector spin chirality $\kappa_{1x}(H_x)$ of the ground state changes abruptly to the value κ_{1x}=0 at H_{LC} since κ(S=3/2)=0.

In the transverse magnetic field H_x, the scalar chirality is equal to zero, χ=0.

In the isosceles trimer (Fig. 2), the vector spin chirality for the states with M=-1/2 in magnetic field H=H_z has the form κ_z = |d_z|/Δ, κ_z' = -|d_z|/Δ, Δ=(δ^2+d_z^2)$^{1/2}$, δ=½(J_{12}-J_{23}). The Heisenberg δ–distortion reduces the exchange symmetry of the system, destroys the spin chirality and, together with d_z, determines the degree κ_z=|d_z|/Δ of the positive [negative] chirality of the states of the isosceles DM clusters. For G_z<0, the two lowest states with M=-1/2 in Fig 2 are characterized by the positive κ_{1z}^-=0.87 and negative κ_{2z}^-=-0.87 vector chirality, respectively. The dominant positive chiral GS (G_z<0) in Fig. 2 corresponds to the large tunneling gap Δ_{12}' in the ground branch at H_{LC1} and small gap Δ_{23}' in the excited branch at H_{LC2}. The dominant negative chiral GS (G_z>0) corresponds to small tunneling gap Δ_{12}' in the ground branch at H_{LC1} and large gap Δ_{23}' in the excited branch at H_{LC2}. Since the intensities of the inter- and intra-doublet EPR transitions in Fig. 2 have the form W_{14}=W_{23}=(d_z/2Δ)^2, W_{12}= W_{34}=(δ/2Δ)^2, there is a direct correlation between the spin chirality κ_z in the isosceles cluster, on the one side, and the intensities of the EPR and INS (see Eqs (6), (7)) transitions, on the other side,

$$W_{14}=W_{23}=\kappa_z^2/4;\; W_{12}= W_{34}=(1- \kappa_z^2)/4. \tag{13}$$

$$S_I= 1/2+(\kappa_z^2/6)[1-4\cos(\mathbf{QR}_{23})], \tag{14}$$

$$S_{II}= 1/3[1-\cos(\mathbf{QR}_{12})]-(\kappa_z^2/6)[1-4\cos(\mathbf{QR}_{23})];$$

$$S_I'= 1/2+(\kappa_z^2/18)[1-4\sin(QR)/QR],\; S_{II}'=1/3[1-\sin(QR)/QR]-(\kappa_z^2/18)[1-4\sin(QR)/QR].$$

The degree of chirality κ_z=|d_z|/Δ may be determined from the EPR and INS experiments. The scalar chirality $\chi(H_z)$ of the M=-1/2 state in Fig.4 have the opposite sign in comparison with κ_z, χ_{1z}=-|d_z|/Δ, χ_{2z} = d_z|/Δ.

In the case of the transverse magnetic field, H=H_x, the field and deformation dependence of the vector chirality of the isosceles Cu_3 cluster has the form

$$\kappa_{1x}=|d_z|/[(\delta+h_x)^2+d_z^2]^{1/2}\,,\quad \kappa_{2x}=|d_z|/[(\delta-h_x)^2+d_z^2]^{1/2}. \tag{15}$$

The vector chirality correlate with the intensities of the inter-doublet EPR transitions $(1\rightarrow4)_x$ and $(2\rightarrow3)_x$ in the transverse field $H=H_x$,

$$W'_{14}(H_\perp) = \kappa_{1x}^2 / 4, \qquad W'_{23}(H_\perp) = \kappa_{2x}^2 / 4. \tag{16}$$

The scalar chirality in the field $H_\perp$ is equal to zero.

The operator of the vector chirality $\boldsymbol{K}_z$ describes the spin chirality of the S=1/2 states in the Cu_3 and V_3 nanomagnets, its field, orientation and distortion dependence. The operator of the scalar chirality $\boldsymbol{C}_z$ describes the pseudoorbital moment $\chi=M_L$; $\chi=0$ in the transverse field $H_\perp$.

6. Conclusion

The DM exchange results in i) the Q-dependence of the structure factor S_I of the INS intra-doublet transition I and ii) redistribution of the Q-independent (Q-dependent) parts of the intensities factors of the intra-doublet I and doublet-doublet II INS transitions with the conservation of the summary Q-independent (Q-dependent) intensities of these two transitions. For the intra-doublet and doublet-doublet transitions, the changes and redistribution of the intensities of the INS transitions I and II, on the one hand, and the intensities of the EPR transitions, on the other hand, have the same origin: they are controlled by the DM exchange and distortions (the $[G_z/\Delta]^2$ terms). The joint consideration of the INS and EPR transitions in the V_3 clusters in the Heisenberg plus DM exchange models shows that the Q-dependence of the INS transitions, peak positions and EPR transitions in the V_3 ring of V_{15} quantum molecular magnet as well as EPR transitions in the V_3 and Cu_3 nanomagnets can be explained in the isosceles model with the DM exchange.

The vector chirality model describes the field, deformation and orientation dependence of the spin chirality κ_n of the Cu_3 and V_3 nanomagnets with DM exchange. The spin chirality is formed by the DM interaction, depends on the sign of the DM parameter G_z and is equal to zero for the pure Heisenberg clusters. The DM exchange and distortions determine the degree of chirality $\kappa_n<1$ in the isosceles clusters. The spin chirality κ_n correlates with the intensities of the EPR and INS transitions.

References

[1]. Gatteschi D., Sessoli R., Villain J., Molecular Nanomagnets, Oxford University Press, New York, 2006.
[2]. (a) Bertaina S., Gambarelli S., Mitra T., Tsukerblat B., Müller A., Barbara B., Nature, 453 (2008) 203. (b) Lehmann J., Gaita-Arino A., Coronado E., Loss D., Nature Nanotechnology, 2 (2007) 312.
[3]. Carretta S., Santini P., Amoretti G., Troiani F., Affronte M., Phys. Rev B 76 (2007) 024408.
[4]. Bogani L., Wernsdorfer W., Nature Materials, 7 (2008) 179.
[5]. Solomon E. I., Sandaram U.H., Machonkin T.E., Chem. Rev. 96 (1996) 2563.
[6]. Tsukerblat B.S., Belinsky M.I., *Magnetochemistry and Radiospectroscopy of Exchange Clusters*, Shtiintsa, Kishinev, USSR, 1983.
[7]. Tsukerblat B.S., Belinsky M.I., Fainzilberg V.E., Sov. Sci. Rev. B. Chem. 9 (1987) 337.
[8]. Dzyaloshinsky I., J. Phys. Chem. Sol. 4 (1958) 241.
[9]. Moriya T., Phys. Rev. Lett. 4 (1960) 228; Phys. Rev. 120 (1960) 918.
[10]. Tsukerblat B.S., Novotortsev V.M., Kuyavskaya B.Ya., Belinsky M.I., Ablov A.V., Bazhan A.N., Kalinnikov V.T., Sov. Phys. JEPT Lett. 19 (1974) 277.
[11]. Tsukerblat B.S., Kuyavskaya B.Ya., Belinsky M.I., Ablov A.V., Novotortsev V.M., Kalinnikov V.T., Theor. Chim. Acta. 38 (1975) 131.
[12]. (a) Padilla J., Gatteschi D., Chaudhuri P., Inorg. Chim. Acta 260 (1997) 217. (b) A. Bencini, D.Gatteschi, EPR of Exchanged-Coupled Systems, Springer, Berlin, 1990.
[13]. Ferrer S., Lloret F., Bertomeu, Alzuel G., Borras J., Garsia-Granda S., Gonsalez M., Haasnoot G., Inorg. Chem. 41 (2002) 5821. I.
[14]. Liu X., Miranda M.H, McInnes T.J.L., Kilner C.A., Harlow M.A. , Dalton. Trans. (2004) 59.
[15]. (a) J.Yoon, L.M. Mirica, T. D. P. Stack, E. I. Solomon, J. Am. Chem. Soc.126 (2004) 12586. (b) J. Yoon, E. I. Solomon, Coord. Chem. Rev. 251 (2007) 379.
[16]. Afrati T., Dendrinou-Samara C., Raptopoulou C., Terzis A., Tangoulis V., Kessissoglou P., Dalton Trans. (2007) 5156.
[17]. Belinsky, M.I. *Inorg. Chem*. 2004, *43*, 739.
[18]. (a) Belinsky M.I., Inorg. Chem. 47 (2008) 3521. (b) M.I. Belinsky, Inorg. Chem. 47 (2008) 3532.
[19]. Choi K.-Y., Dalal N.S., Reyes A.P., Kuhns P.L., Matsuda Y.H., Nojiri H., Mal S.S., Kortz U., Phys. Rev. *B* 77 (2008) 024406.
[20]. Choi K.-Y., Matsuda Y.H., Nojiri H., Kortz U., Hussain F., Stowe A.C., Ramsey C., Dalal N.S., Phys.Rev.Lett. 96 (2006) 107202.
[21]. Trif M., Troiani F., Stepanenko D., Loss D., Phys.Rev Lett. 101 (2008) 217201.

[22]. (a) Yamase, T.; Ishikawa, E.; Fukaya, K.; Nojiri, H.; Taniguchi, T.; Atake, T. *Inorg. Chem.* 2004, *43*, 8150. (b) Nojiri, H.; Ishikawa, E.; Yamase, T. *Progr. Theor. Phys. Suppl*.No159, 2005, 292.
[23]. (a) Chiorescu I., Wernsdorfer W., Müller A., Bogge H., Barbara B., Phys.Rev. Lett. 84 (2000) 3454. (b) Chiorescu I., Wernsdorfer W., Barbara B., Müller A., Bogge H., J.Magn.Magn.Mater. 221 (2000) 103. (c) Barbara B., J. Mol. Struct. 656 (2003) 135.
[24]. (a) Chiorescu I., Wernsdorfer W., Müller A., Miyashita S., Barbara B., Phys.Rev. B, 67 (2003) 020402. (b) Barbara B., Chiorescu I., Wernsdorfer W., Bogge H., Müller A., Prog. Theor. Phys.Suppl. No 145 (2002) 357. (c) Noijri H., Taniguchi T., Ajiro Y., Müller A., Barbara B., Physica B, 346-347 (2004) 216.
[25]. (a) Miyashita S., Nagaosa N. Prog. Theor. Phys. 106 (2001) 533. (b) S. Miyashita, H. De Raedt, K. Michieslsen, Prog. Theor. Phys. 110 (2003) 889.
[26]. (a) Sakon T., Koyama K., Motokawa M., Ajiro Y., Müller A., Barbara B., Physica B, 346-347 (2004) 206. (b) Sakon T., Koyama K., Motokawa M.; Müller A., Barbara B., Ajiro Y., Progr.Theor.Phys. Suppl. No 159, (2005) 302.
[27]. Konstantinidis N.P., Coffey D., Phys.Rev.B 66 (2002) 174426.
[28]. De Raedt H., Miyashita S., Michielsen K., Machida M., Phys.Rev. B, 70 (2004) 064401.
[29]. (a) Machida M., Iitaka T., Miyashita S., J. Phys.Soc.Jpn., 74 (2005) 107. (b) Machida M., Miyashita S., Physica E, 29 (2005) 538.
[30]. (a) Tarantul A., Tsukerblat B., Müller A., Chem.Phys. Let. 428 (2006) 361. (b) Tsukerblat B., Tarantul A., Müller A., Phys. Lett. 353 (2006) 48.
[31]. (a) Tarantul A., Tsukerblat B., Müller A., Inorg. Chem. 46 (2007) 161. (b) A.Tarantul, B.Tsukerblat, Müller A., J. Chem. Phys. 125 (2006) 054714.
[32]. (a) Tsukerblat B., Tarantul A., Müller A., J. Molec. Structure. 838 (2007) 124. (b) Tarantul A., Tsukerblat B., Müller A., Solid State Sc. 10 (2008) 1814.
[33]. Kajiyoshi K., Kambe T., Mino M., Norjiri H., Kögerler P., Luban M., J. Magn. Magn.Mater. 310 (2007) 1203.
[34]. Chaboussant G., Ochsenbein S.T., Seiber A., Güdel H.-U., Mutka H., Müller A., Barbara B., Europhys.Lett. 66 (2004) 423.
[35]. Borras-Almenar J.J., Clemente-Juan J.M., Coronado E., Tsukerblat B.S., Inorg. Chem. 38 (1999) 6081.
[36]. Haraldsen J.T., Barbes T., Musfeldt J.L., Phys.Rev. B 71 (2005) 064403.
[37]. (a) Waldmann O., Güdel H-U., Phys. Rev. B 72 (2005) 094422. (b) Waldmann O., Bircher R., Carver G., Seiber A.; Güdel H-U., Mutka, H. Phys. Rev. B 75 (2007) 174438.
[38]. (a) Grohol D., Matan K., Cho J.-H., Lee S.H., Lynn J.W., Nocera D.G., Lee J.S., *Nature*, (2005) 323. (b) Helton J.S., *et al Phys. Rev. Lett*. 98 (2007) 107204. (c) H. Kawamura, J. Phys.:Condens. Matter 10 (1998) 4707.
[39]. Belinsky M. I., Chem Phys., 2009, In press.